

Supporting information

Evidence for core oxygen dynamics and exchange in metal oxide nanocrystals from in situ ^{17}O MAS-NMR

Yohan Champouret, Yannick Coppel,* and Myrtil L. Kahn*

Characterization by Transmission Electron Microscopy (TEM)

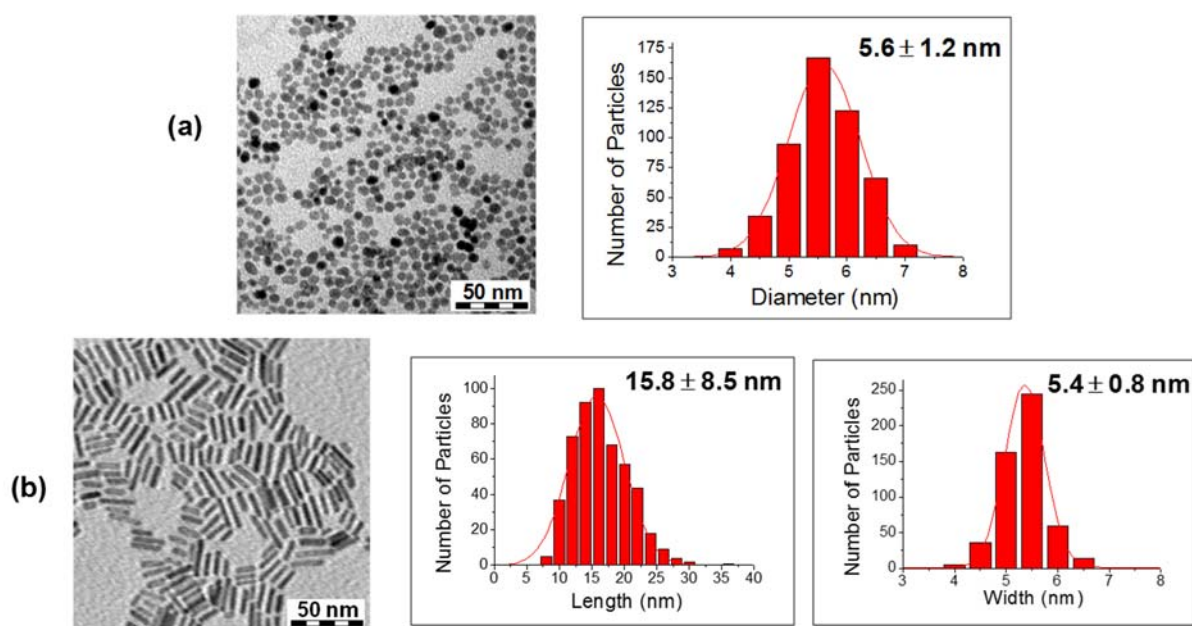


Figure S1: TEM images of (a) isotropic NCs (Sample 1) and (b) nanorods (Sample 2) with their respective size-distribution histogram.

¹³C CP/MAS NMR spectra of isotropic (Sample 1) and nanorods (Sample 2) ZnO NCs before and after washing

The ¹³C CP/MAS spectra recorded after the washing procedure of Sample 1 and Sample 2 showed only ¹³C resonances characteristic of the most strongly bound amine ligand (Figure S2-1 and Figure S2-2).

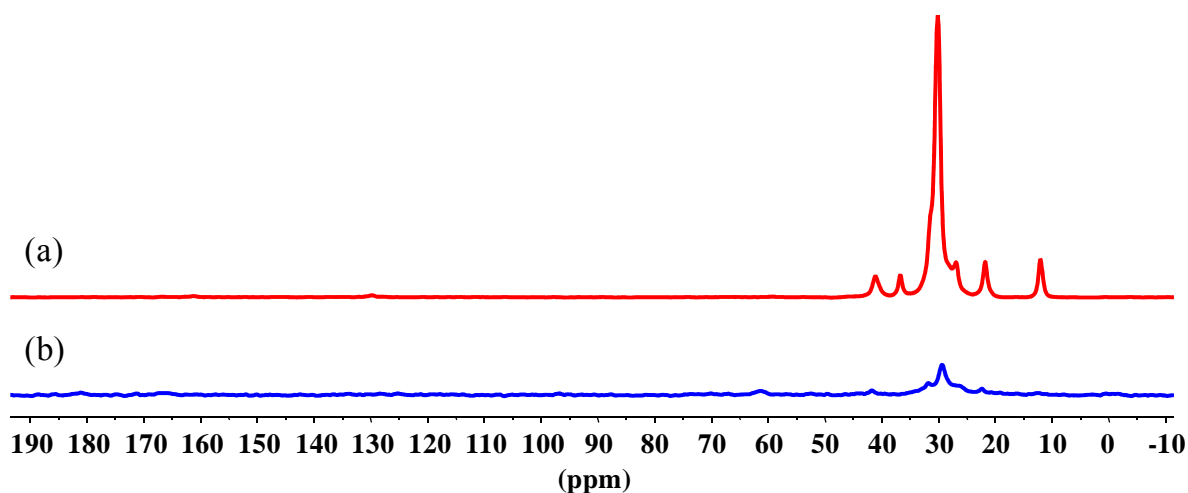


Figure S2-1: ¹³C CP/MAS spectra of isotropic ZnO NCs (Sample 1) synthesized with 1 eq. of DDA ligand before (a) and after washing procedure (b).

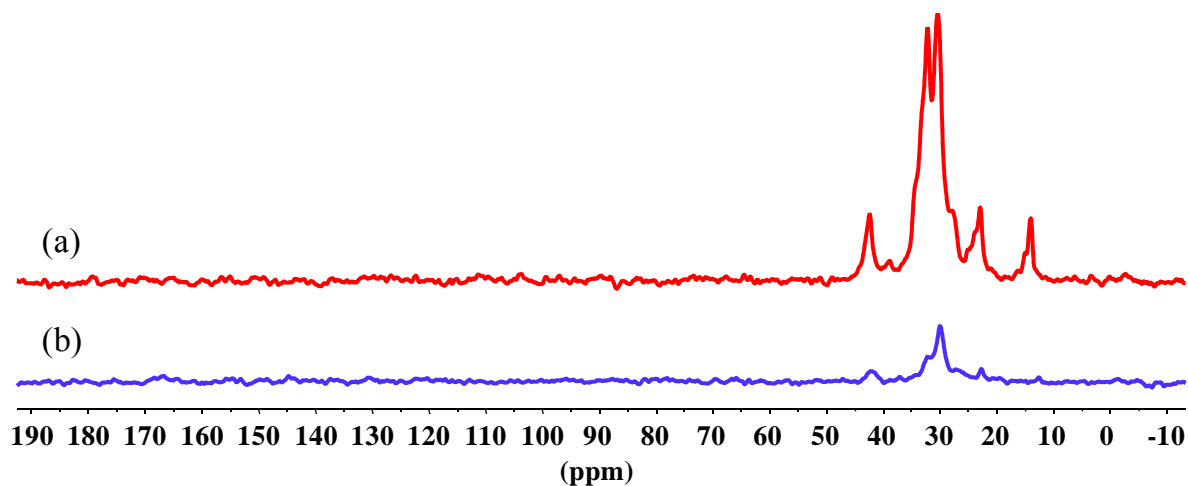


Figure S2-2: ¹³C CP/MAS spectra of nanorods ZnO NCs (Sample 2) synthesized with 2 eq. of DDA ligand before (a) and after washing procedure (b).

1D ^{17}O and 1D T_1 -filtered ^{17}O MAS NMR spectra of isotropic (Sample 1) and nanorods (Sample 2) ZnO NCs.

Few minutes after the water introduction, the ^{17}O spectra displayed only a water signal at 0.0 ppm. Over time, new signals appeared in the spectral area between -15 to -50 ppm but with a signal growth kinetic difficult to follow because of the presence of the strong ^{17}O water signal. ^{17}O T_1 of water and of the three main ZnO NCs resonances observed at -17.6, -23.6 and -29.4 ppm were measured with values of 5 ms, 2.6 s, 1.0 s and 0.8 s, respectively. Due to the difference of several orders of magnitude between the T_1 of water (5 ms) and the ones of ZnO oxygens (2.6 – 0.8 s), 1D T_1 -filtered ^{17}O MAS (*cf experimental section*) spectra could be acquired with good suppression of water signal without affecting the ZnO signal intensities (Figure S3-1 and Figure S3-2).

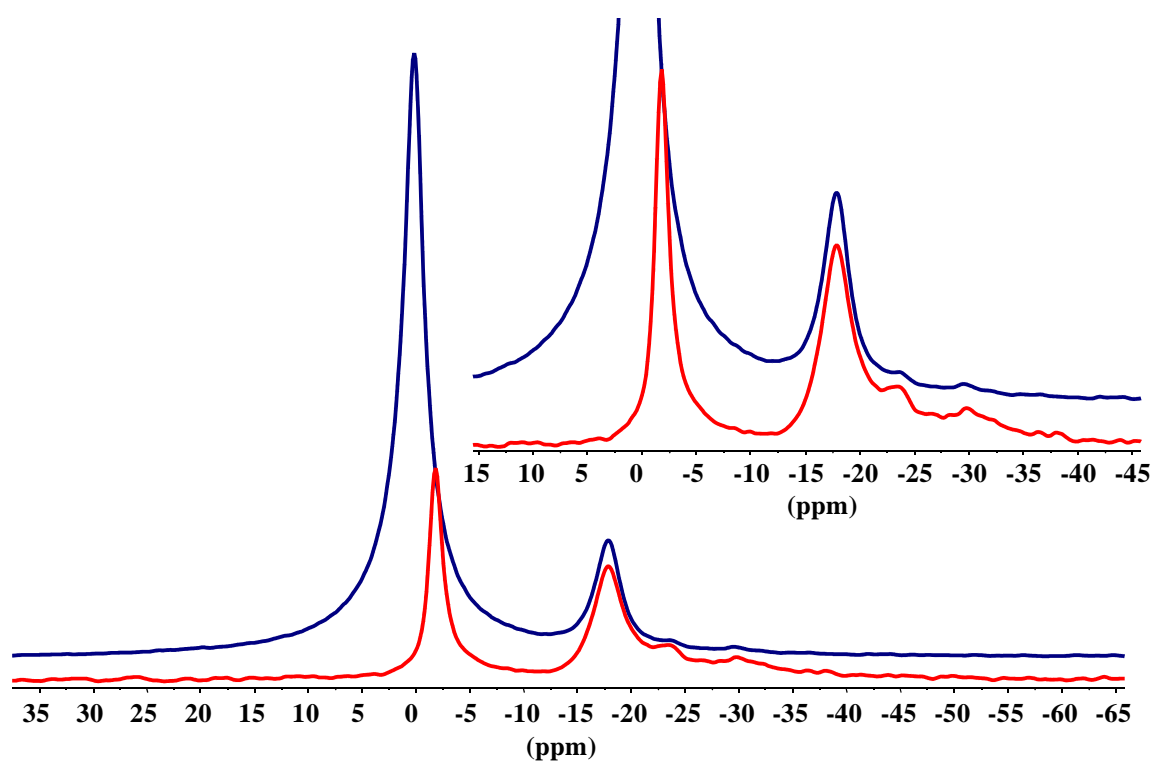


Figure S3-1: 1D ^{17}O (blue) and 1D T_1 -filtered ^{17}O (red) MAS of isotropic ZnO NCs (Sample 1) exposed in situ to ^{17}O -labeled water for 1 h 40 min. Note that the residual water signal in the 1D T_1 -filtered ^{17}O is shifted compared to the one in the 1D ^{17}O . It indicates the presence of different kind of water molecules with different mobilities and longer T_1 relaxation times (see also below, Figures S4-1 and S17b).

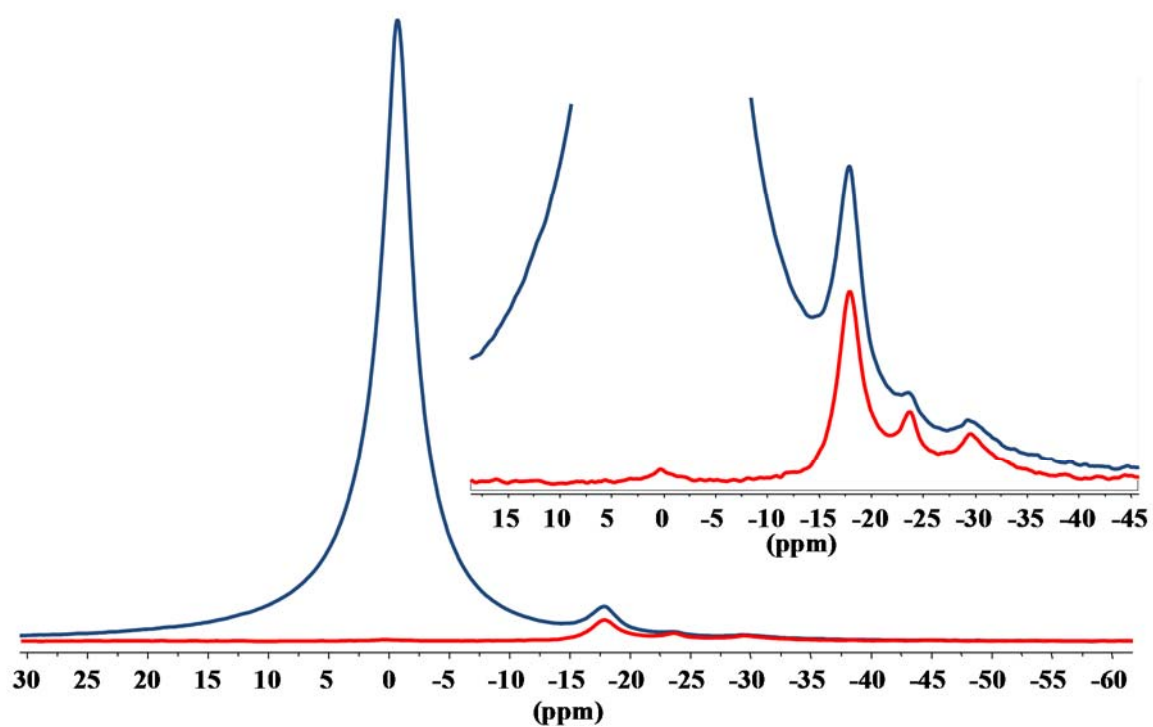


Figure S3-2: 1D ^{17}O (blue) and 1D T_1 -filtered ^{17}O (red) MAS of nanorods ZnO NCs (Sample 2) exposed in situ to ^{17}O -labeled water for 26 h.

1D T_1 -filtered ^{17}O MAS NMR spectra of isotropic (Sample 1) and nanorods (Sample 2) ZnO NCs in the presence of ^{17}O -enriched water over time.

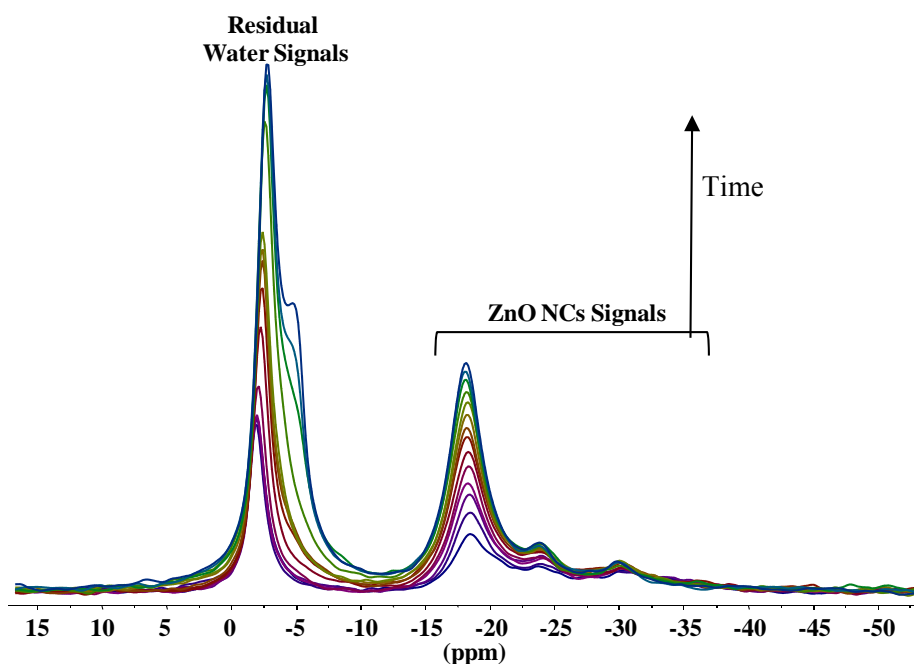


Figure S4-1: 1D T_1 -filtered ^{17}O MAS spectra of isotropic ZnO NCs (Sample 1) exposed to ^{17}O -enriched water between 20 min and 20 h.

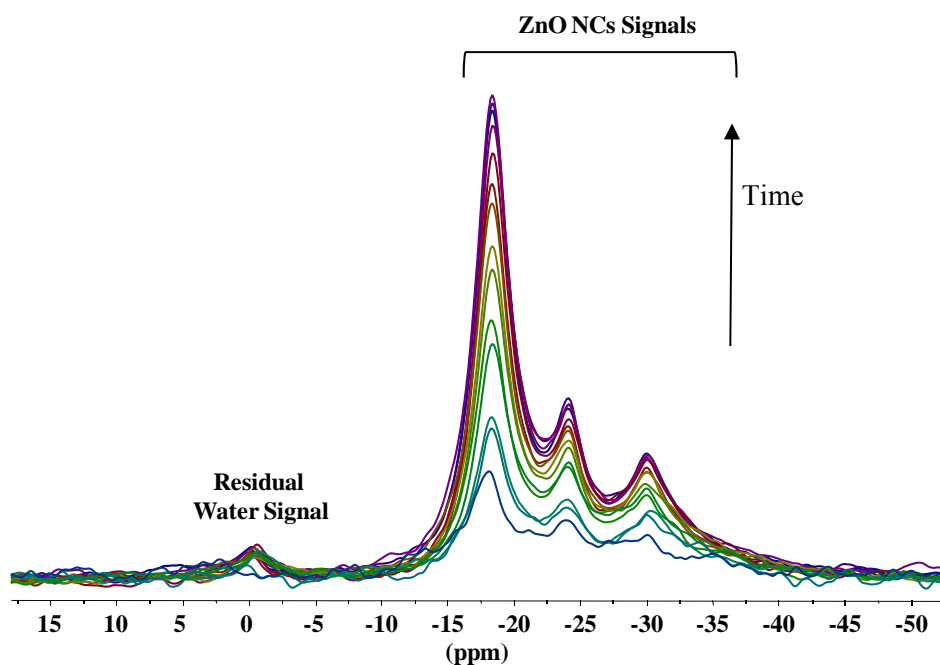


Figure S4-2: 1D T_1 -filtered ^{17}O MAS spectra of nanorods ZnO NCs (Sample 2) exposed to ^{17}O -enriched water between 3 h and 26 h.

Full ^{17}O MAS NMR spectra of isotropic ZnO NCs (Sample 1) showing the satellite transition spinning sidebands and their simulation.

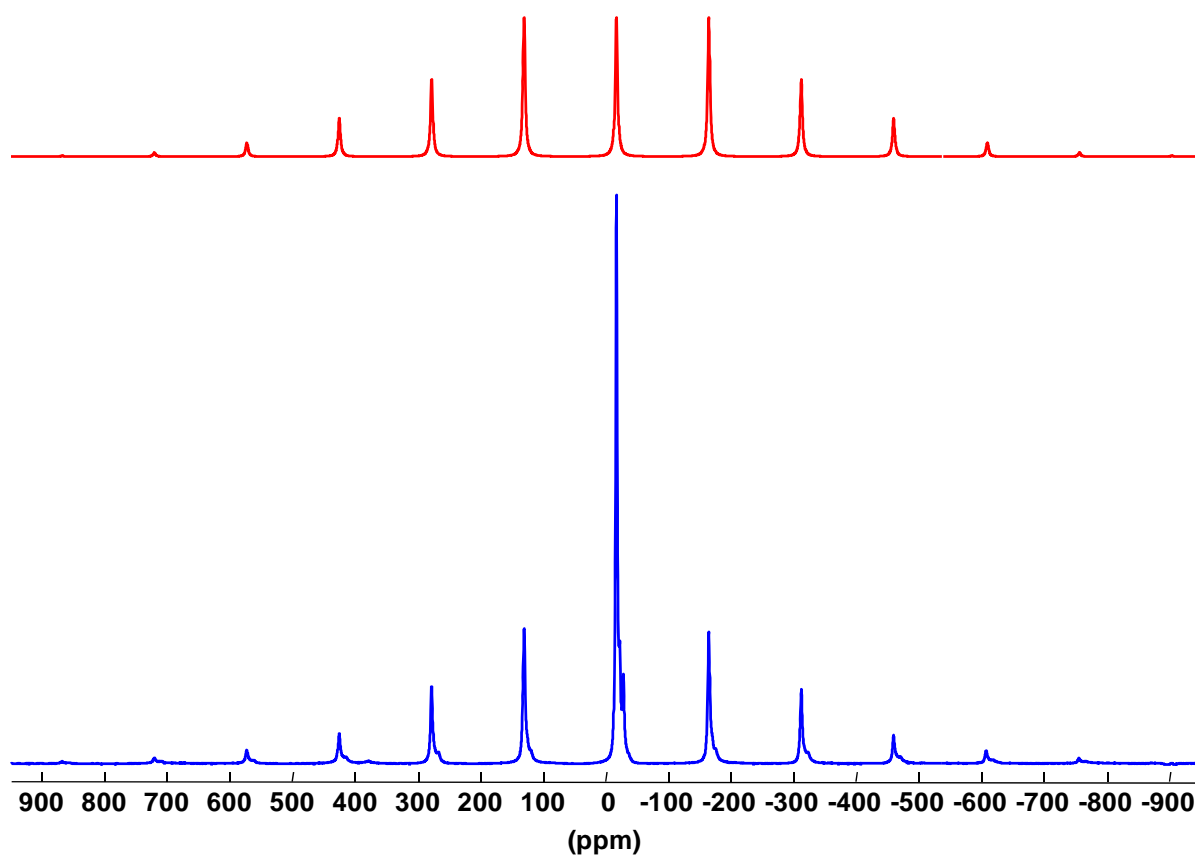


Figure S5: ^{17}O MAS spectra (8 kHz) of isotropic ZnO NCs (Sample 1) exposed to ^{17}O -enriched water for 24 h and vacuum dried for one night to remove ^{17}O water signal (in blue). The $\pm 3/2 \leftrightarrow \pm 1/2$ and $\pm 5/2 \leftrightarrow \pm 3/2$ satellite transitions of the ^{17}O signal at -17.7 ppm were simulated and summed with the DMFIT software by using a Gaussian/Lorentzian function and a quadrupolar coupling constant of 130 kHz (in red). This value is in accordance with the value of 130 kHz observed for a ZnO powder by Oldfield and coworkers.^[1] The intensity of satellite transitions at the isotropic shift ($n=0$) was found to be of the same intensity than the $n=\pm 1$ spinning sidebands. The intensity of the $n=0$ spinning sidebands of the satellite transitions were deduced from the $n=\pm 1$ spinning sidebands in the following simulation.

Experimental and simulation of central transition and first spinning sidebands of the satellite transition of ^{17}O MAS NMR spectra of isotropic ZnO NCs (Sample 1)

D'Espinose de Lacaillerie *et al.*^[2] showed that a “large enough” coordination number that allows the use of the Czjzek model should be at least equal to four for the probe nuclei. Good fitting of the ^{17}O spectra could be therefore obtained with this model since oxygen anion are tetrahedrally coordinated in the wurtzite structure of ZnO.

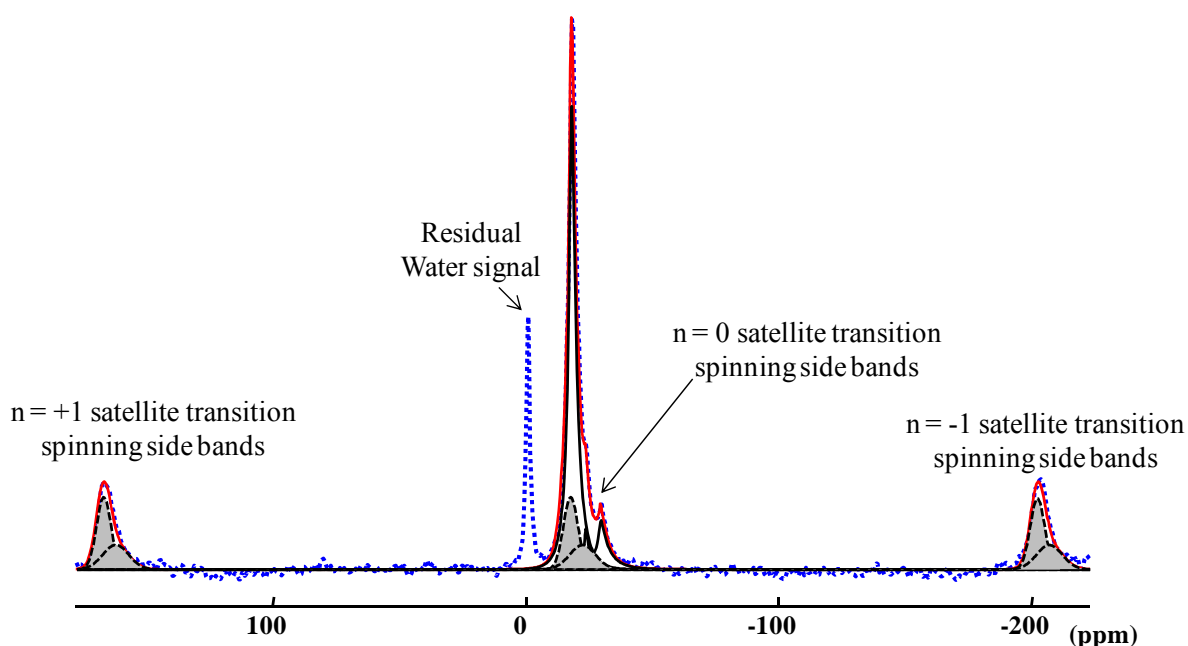


Figure S6: 1D T_1 -filtered ^{17}O (blue) MAS (spinning rate 10 kHz, relaxation delay of 20 s) of isotropic ZnO NCs (Sample 1) in the equilibrium state of the isotope exchange experiments. Central transition (in black) were simulated with the Czjzek model. The satellite transitions should also have been modeled with 3 components by using the Czjzek model. However the complete simulation of the ^{17}O spectra (central and satellite transitions) with the Czjzek model was very time-consuming and difficult to perform for the kinetic study (see below). As the satellite transitions contribution to the center band signal is limited (about 25%), we speed up the simulations by replacing the fitting of the satellite transitions with 3 components using the Czjzek model by a fitting with two Gaussian/Lorentzian functions that gave a satisfactory representation. The intensity of the $n=0$ spinning side bands of the satellite transitions were deduced from the $n=\pm 1$ spinning sideband ones (see Figure S5). The $n= -1, 0$ and 1 spinning sidebands of the satellite transitions are shown in dashed line and filled in grey.

1D T_1 -filtered ^{17}O MAS NMR spectra of isotropic (Sample 1) and nanorods (Sample 2) ZnO NCs compared to simulated spectra.

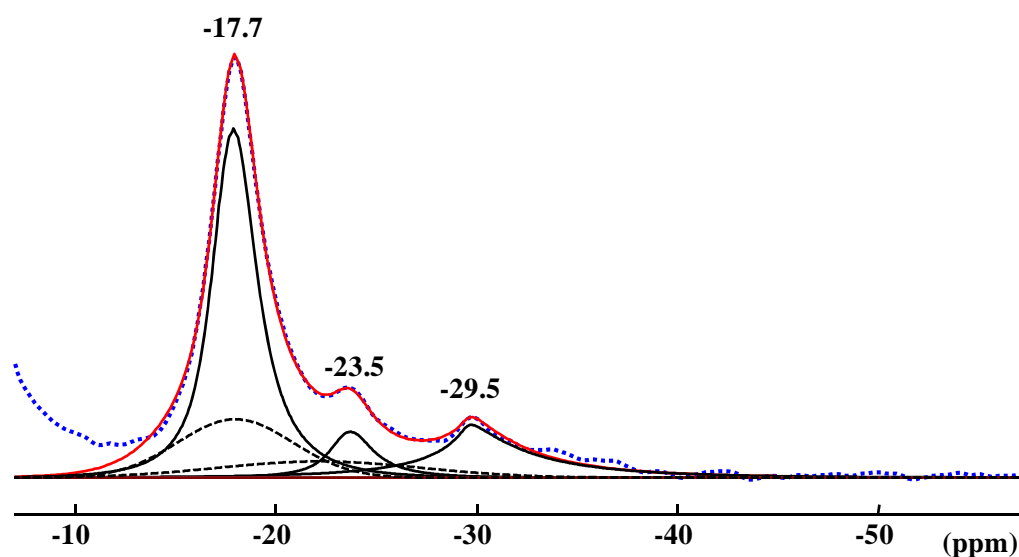


Figure S7-1: 1D T_1 -filtered ^{17}O (blue) MAS of isotropic ZnO NCs (Sample 1) exposed in situ to ^{17}O -labeled water for 17 h compared to simulated spectra (in red). Central transition (in black) were simulated with the Czjzek model. The $n=0$ spinning side bands of the satellite transition are shown in dashed line.

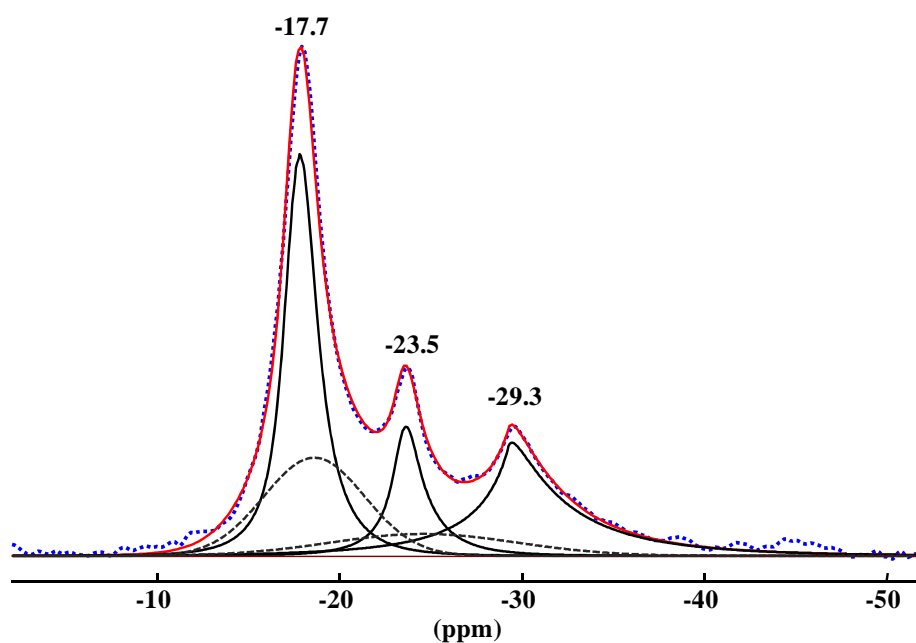


Figure S7-2: 1D T_1 -filtered ^{17}O (blue) MAS of nanorods ZnO NCs (Sample 2) exposed in situ to ^{17}O -labeled water for 26 h compared to simulated spectra (in red). Central transition (in black) were simulated with the Czjzek model. The $n=0$ spinning side bands of the satellite transition are shown in dashed line.

Evolution of peak integrals of the -17.7(high), -23.5(medium) and -29.4(low) ppm resonances of Sample 1 (Fig S8-1) and Sample 2 (Fig S8-2) in function of exposition time to H₂O-enriched in ¹⁷O. The fitting curves are represented by the dashed lines (---) using the equation $I(t)=I(\infty)[1 - \exp\{-k.t\}]$.

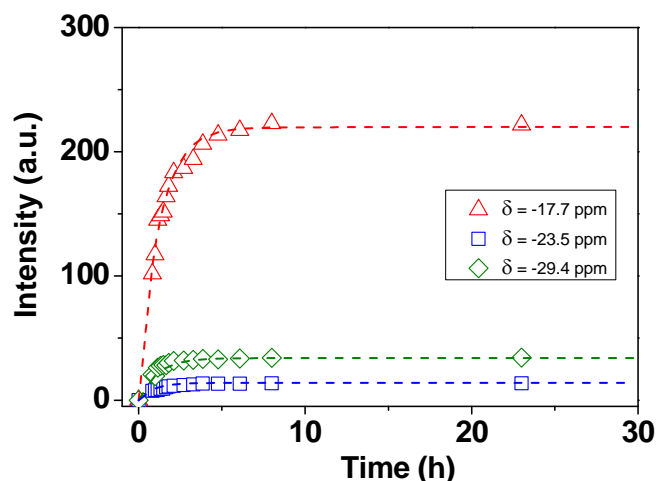


Figure S8-1: Areas $\delta = -17.7(\pm 0.1)$ ppm (high, Δ), $\delta = -23.5(\pm 0.2)$ ppm (medium, \square), $\delta = -29.4(\pm 0.2)$ ppm (low, \diamond) of Sample 1 in function of exposition time to H₂O-enriched in ¹⁷O. The fitting curves are represented by the dashed lines (---) using the equation $I(t)=I(\infty)[1 - \exp\{-k.t\}]$.

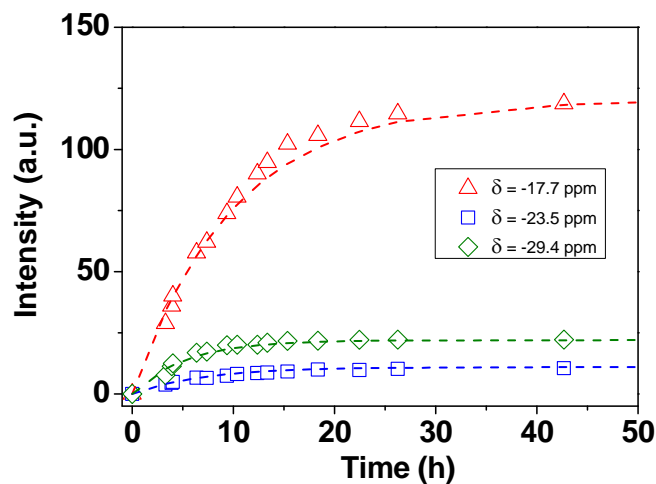


Figure S8-2: Areas $\delta = -17.7(\pm 0.1)$ ppm (high, Δ), $\delta = -23.5(\pm 0.2)$ ppm (medium, \square), $\delta = -29.4(\pm 0.2)$ ppm (low, \diamond) of Sample 2 in function of exposition time to H₂O-enriched in ¹⁷O. The fitting curves are represented by the dashed lines (---) using the equation $I(t)=I(\infty)[1 - \exp\{-k.t\}]$.

1D T_1 -filtered ^{17}O MAS spectra of ZnO NCs in the equilibrium state: isotropic (Sample 1), nanorods (Sample 2), isotropic submitted to 2 (Sample 3) and 6 (Sample 4) cycles of long water exposition and vacuum drying.

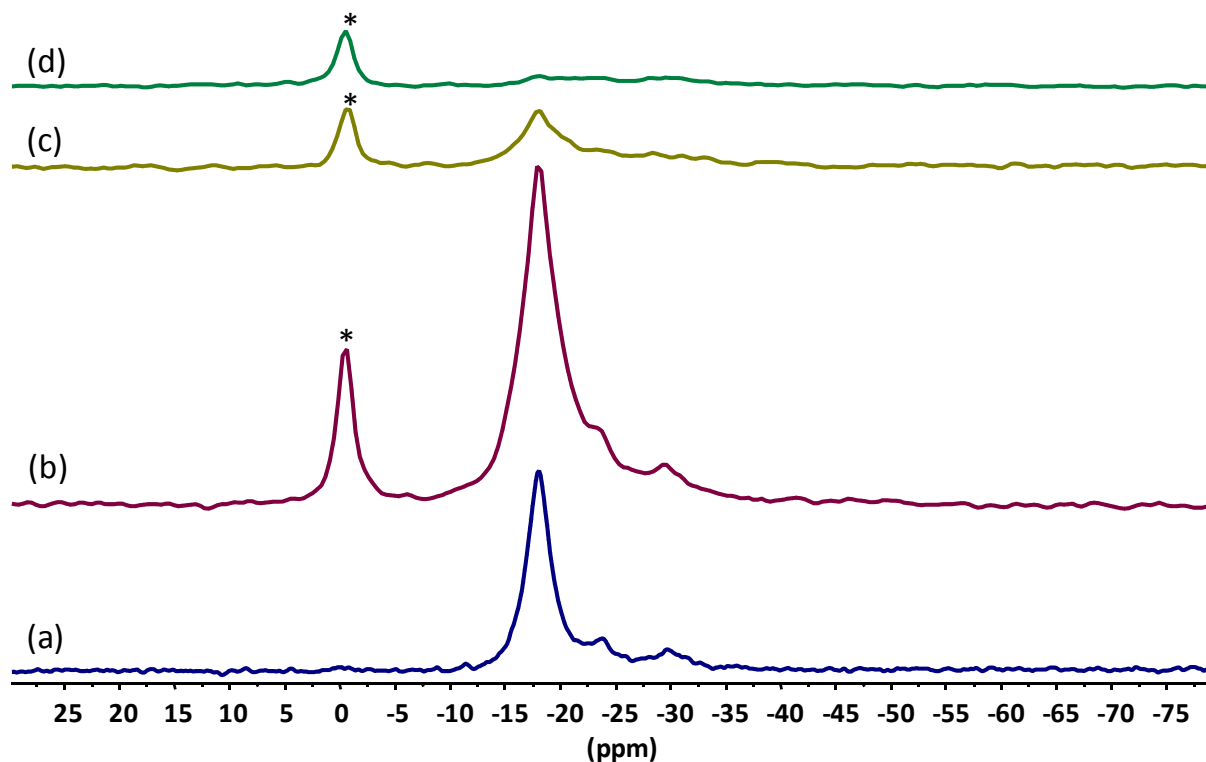


Figure S9: 1D T_1 -filtered ^{17}O MAS spectra (relaxation delay of 20 s) of ^{17}O -exchanged ZnO NCs in the equilibrium state of the isotope exchange experiments: nanorods (Sample 2) (a), isotropic (Sample 1) (b) isotropic submitted to 2 (*vide infra*, Sample 3, c) and 6 (*vide infra*, Sample 4, d) cycles of long water exposition and vacuum drying. * Residual water signal. Sample 1, 3 and 4 of isotropic ZnO NCs originate from the same synthesis batch.

Preparation and TEM analysis of isotropic ZnO NCs enriched in ^{17}O (Sample 1')

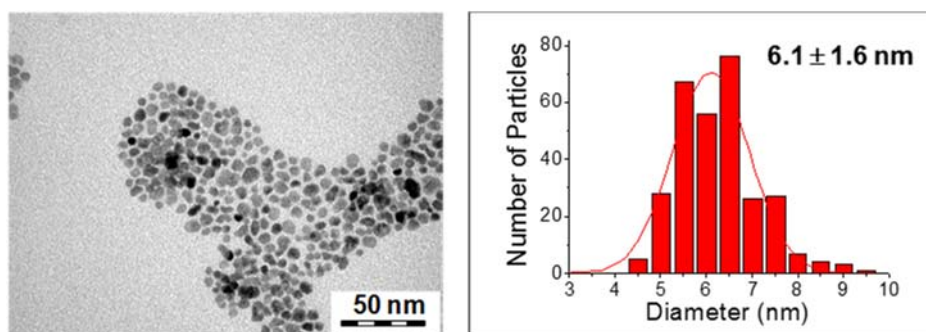


Figure S10: TEM images of isotropic ZnO NCs enriched in ^{17}O (Sample 1') with its size-distribution histogram.

^{17}O MAS NMR spectra of vacuum dried isotropic ZnO NCs (Sample 1') synthesized with ^{17}O -enriched water

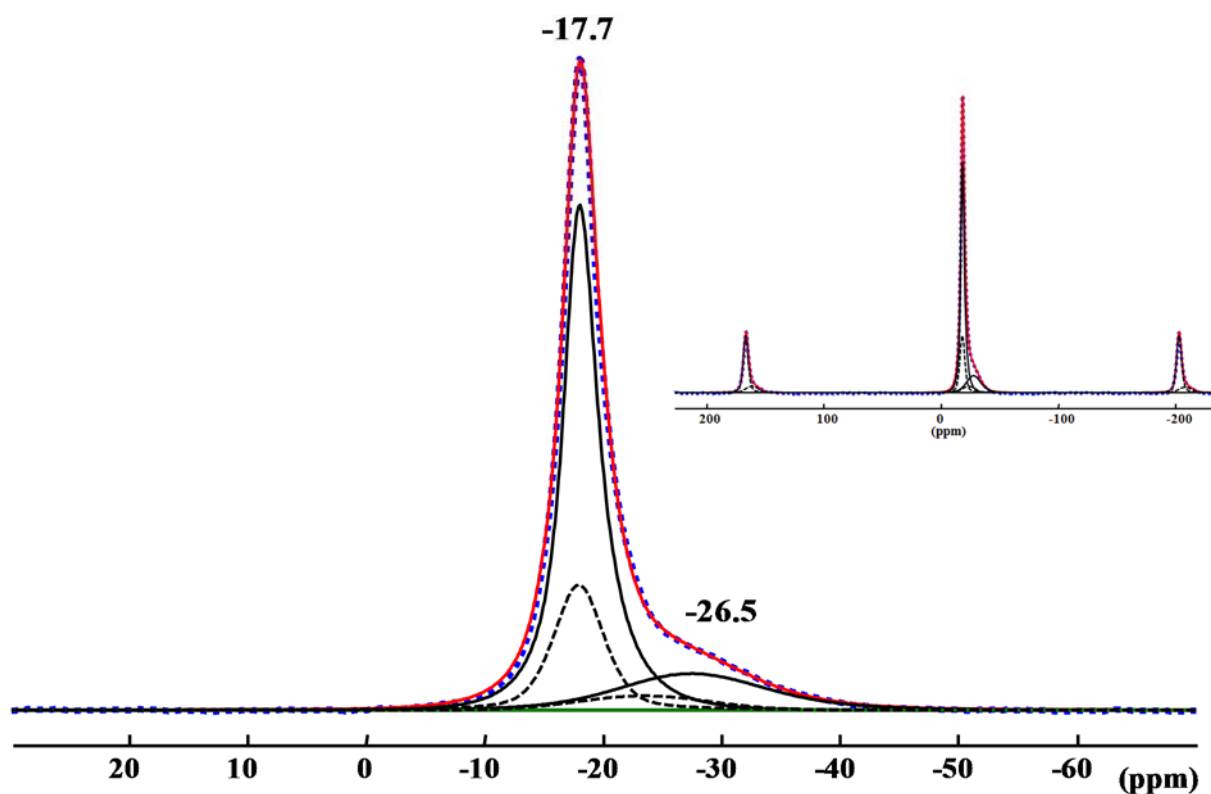


Figure S11: ^{17}O MAS spectra (blue) of vacuum-dried ^{17}O -synthesized isotropic ZnO NCs (Sample 1'). Central transition (in black) were simulated with the Cjzek model. The n = 0 spinning sidebands of the satellite transition are shown in dashed line. Insert: Bigger spectral window showing the n = -1, 0 and 1 spinning sidebands of the satellite transition (simulated with two Lorentzian/Gaussian functions).

Determination of the proportion of oxygen atoms located at the basal faces

The % of O atoms in the basal planes, %O(BP), is equal to the ratio between the number of O atoms of the basal planes, O(BP), and the overall number of O atom in a NC, O(Tot).

$$O(BP) = \frac{3}{2} \frac{d^2}{a^2} \quad \text{and} \quad O(Tot) = \frac{3\sqrt{3}}{4} \frac{d^2 L}{a^2 c \cos 30}$$

which leads to

$$\%O(BP) = \frac{2c \cos 30}{\sqrt{3}L} \times 100$$

In the case of isotropic ZnO NCs of ca 6 nm, $d = L = 6$ nm, a and c are the unit cell for hexagonal wurtzite ZnO structure with $a = 0.33$ nm and $c = 0.52$ nm.

Consequently, %O(BP) = 9 %

¹⁷O MAS and ¹⁷O CP/MAS NMR spectra of vacuum dried isotropic ZnO NCs (Sample 1) after being exposed to ¹⁷O-enriched water.

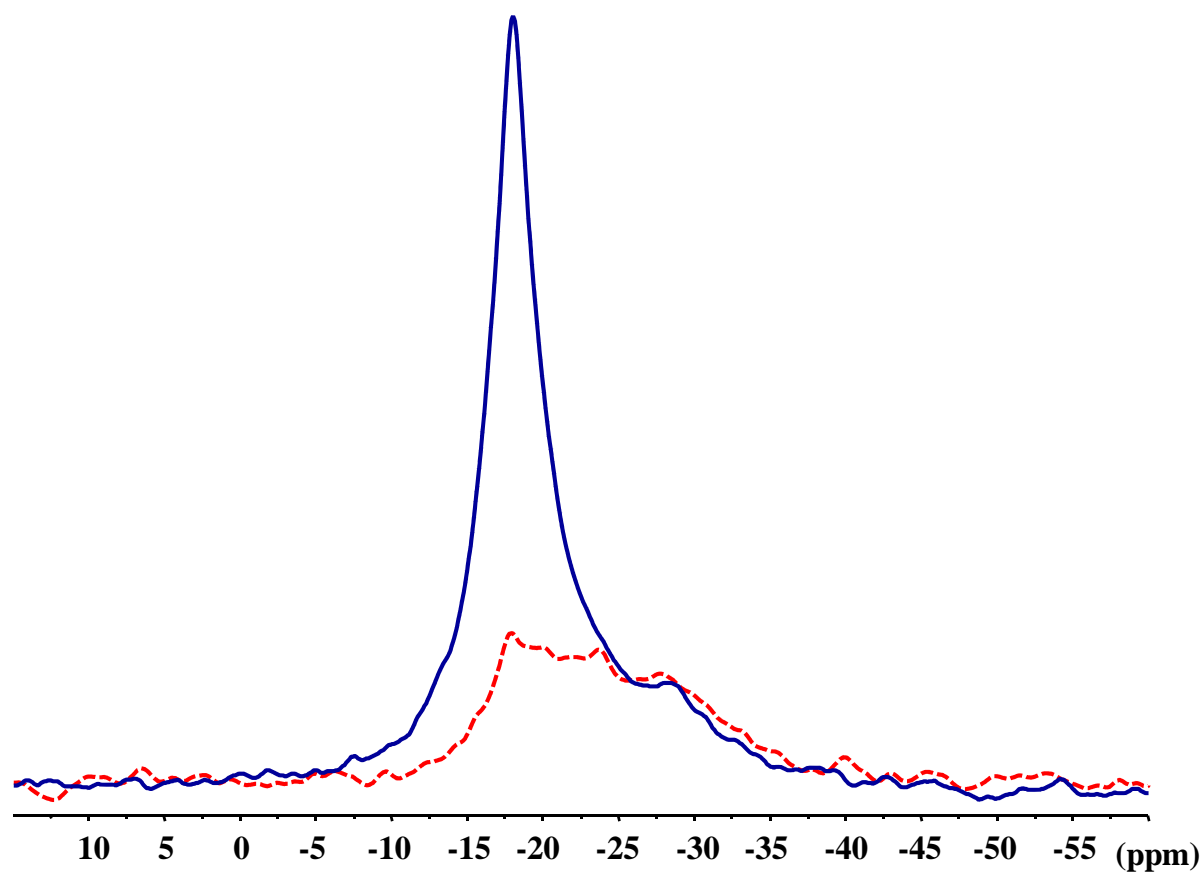


Figure S12: ¹⁷O MAS (solid, blue) and ¹⁷O CP/MAS (contact time 5 ms, dotted, red) of vacuum-dried isotropic ¹⁷O-exchanged ZnO NCs (Sample 1) at the equilibrium state.

^{17}O CP/MAS NMR spectra of vacuum dried nanorods ZnO NCs (Sample 2) after being exposed to ^{17}O -enriched water.

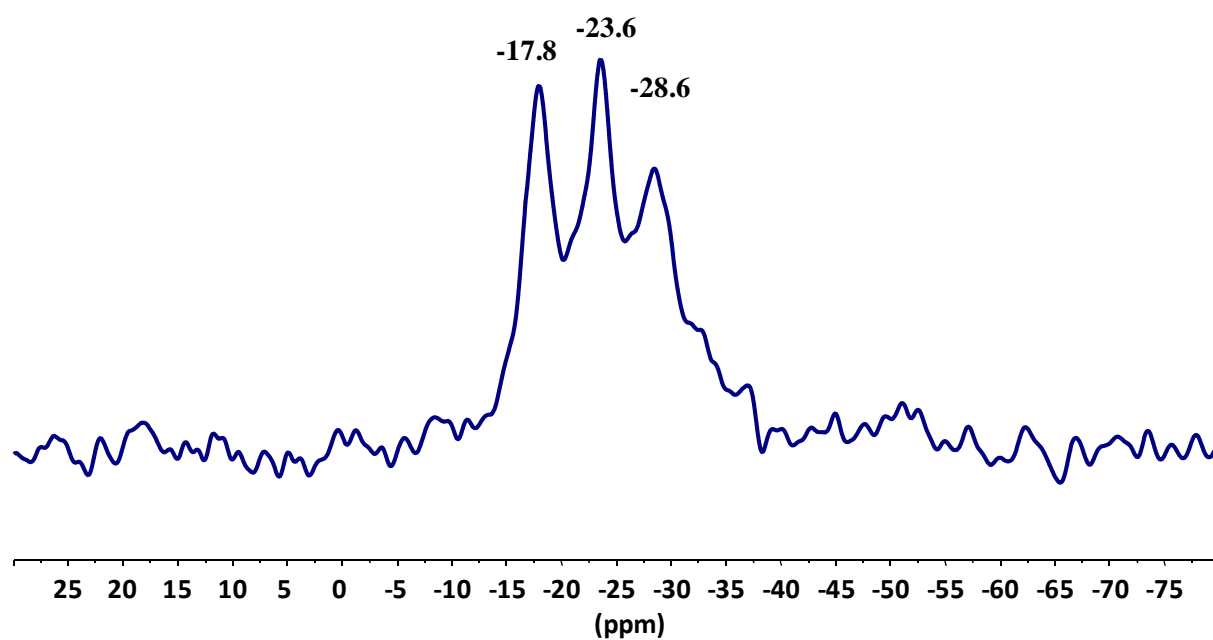


Figure S13: ^{17}O CP/MAS (contact time 5 ms) of vacuum-dried nanorods ^{17}O -exchanged ZnO NCs (Sample 2) at the equilibrium state.

¹⁷O MAS and ¹⁷O CP/MAS NMR spectra of vacuum dried isotropic ZnO NCs (Sample 1') synthesized with ¹⁷O-enriched water.

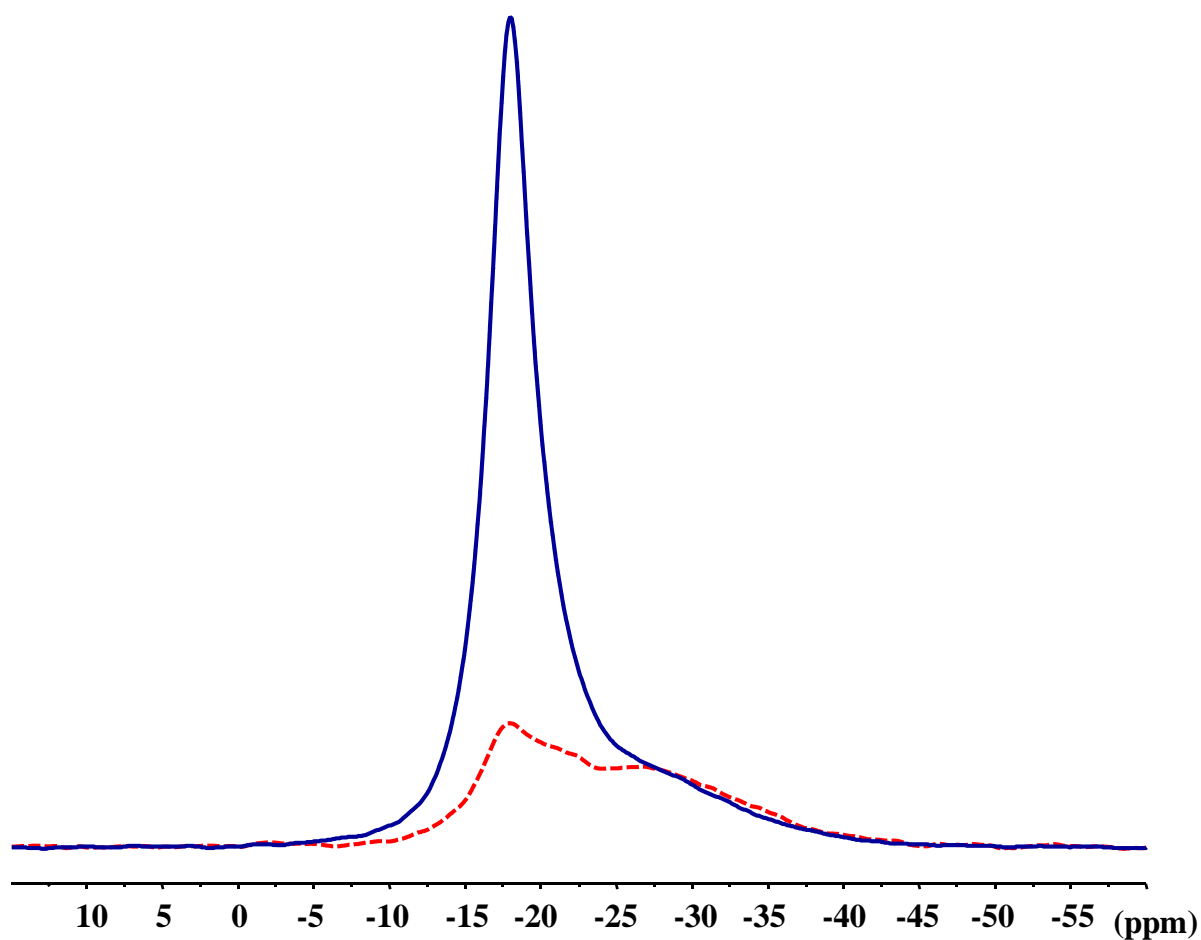


Figure S14-1: ¹⁷O MAS (solid, blue) and ¹⁷O CP/MAS (contact time 5 ms, dotted, red) of vacuum dried isotropic ZnO NCs (Sample 1') synthesized with ¹⁷O-enriched water.

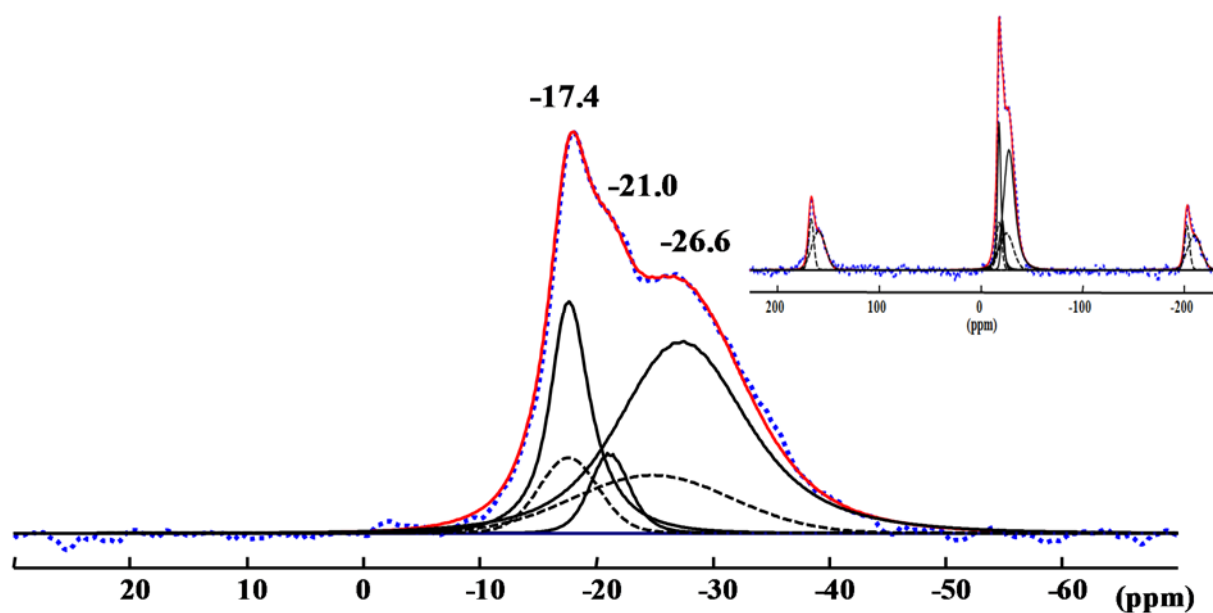


Figure S14-2: ^{17}O CP/MAS spectra (blue) of vacuum-dried ^{17}O -synthesized isotropic ZnO NCs (Sample **1'**). Central transition (in black) were simulated with the Cjzek model. The $n=0$ spinning sidebands of the satellite transition are shown in dashed line. Insert: Bigger spectral window showing the $n= -1, 0$ and 1 spinning sidebands of the satellite transition (simulated with two Lorentzian/Gaussian functions). Three resonances at $-17.4(\pm 0.1)$, $-21.0(\pm 0.2)$ and $-26.6(\pm 0.2)$ ppm with respective population of $27(\pm 3)$, $8(\pm 3)$ and $65(\pm 4)$ % were found.

¹⁷O CP/MAS NMR spectra of isotropic (Sample 1) and nanorods (Sample 2) ZnO NCs exposed to ¹⁷O-enriched water (S15-1); ¹⁷O CP/MAS NMR spectra of isotropic NCs (Sample 1) exposed to ¹⁷O-enriched water over time and after vacuum-drying (S15-2); 1D T₁-filtered ¹⁷O MAS NMR spectra of isotropic (Sample 1) in the equilibrium state before and after vacuum drying (S15-3).

¹⁷O CP/MAS spectra exhibit strong ¹⁷O resonances of ZnO NCs only when the experiments were performed on vacuum-dried samples. When such experiments were performed on non-dried samples, the resulting ¹⁷O CP/MAS spectra showed mostly a strong water signal around 0 ppm characteristic of water molecules with low mobility present in the samples (Figure S15-1). For Sample 1, the ¹⁷O resonances of ZnO NCs with low intensities could be observed in addition to the strong water signal around 0 ppm. But in this case, the resonances of ZnO NCs became weaker as the isotope exchange proceeded, contrary to what it is expected for enrichment experiment (Figure S15-2). This lessening of the transfer of the polarization between ¹H nuclei and ¹⁷O nuclei could be explained by hydrogen diffusion and exchange between the ZnO NCs and clusters of water slowly formed at the surface of the NCs that leads to an averaging of the ¹H-¹⁷O dipolar couplings to zero. This hypothesis is strengthened by the evolution of water residual signal in the 1D T₁-filtered ¹⁷O MAS spectra with time: i) intensity increase and shift (up to -2.6 ppm) of the main residual water signal and ii) the appearance of a new water resonance at -4.6 ppm (inset Figure S15-2). Such residual signals correspond to ¹⁷O atoms of water molecules possessing longer T₁ values compared to the ones of free water molecules that are characteristic of a slow structuration process of the water molecules at the surface of the ZnO NCs. Such an observation is in agreement with theoretical calculations evidencing clustering and formation of monolayer islands of water on ZnO surface,^[3] and to the recent experimental report on ceria.^[4] The hypothesis of the presence of a fast exchange phenomenon between the H atoms of the hydroxyl groups or the interstitial H atoms and the H atoms of the structured water was confirmed by the strong increase of the ¹⁷O ZnO CP/MAS resonances obtained when the sample was dried under vacuum overnight to remove the water molecules (Figure S15-2.b.c). It has also been observed on bone apatite that the ¹H->³¹P (³¹P->¹H) CP kinetics of OH group can strongly fluctuate depending of the OH environments notably through dipole-dipole coupling to surface water or spin-diffusion.^[5, 6]

Note that the vacuum-drying process modified slightly the ¹⁷O MAS spectrum of the isotropic ZnO NCs (Sample 1). This is related to removing of water molecules in interaction with the ZnO surface (hydrogen bonded) and migration of ZnO defects (see below).

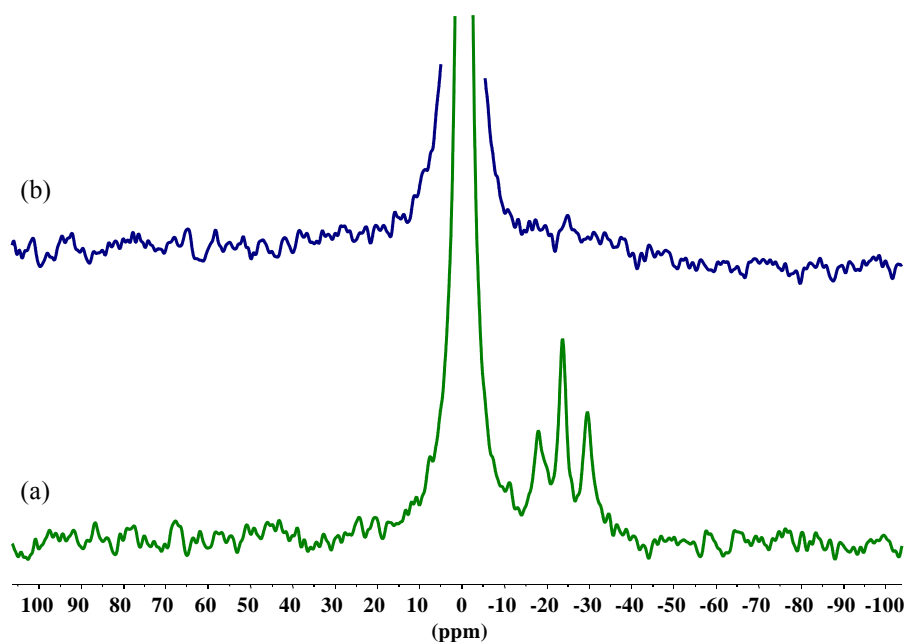


Figure S15-1: ^1H - ^{17}O CP MAS spectra (contact time 5 ms) of isotropic ZnO NCs exposed to ^{17}O -enriched water for 5 h (Sample 1, a) and of nanorods ZnO NCs exposed to ^{17}O water for 6 h (Sample 2, b).

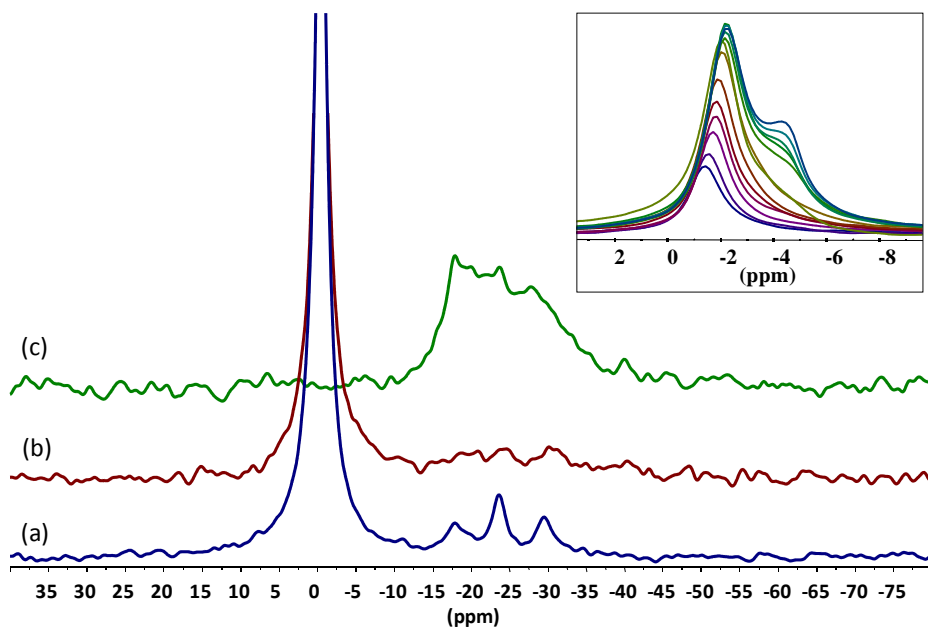


Figure S15-2: ^1H - ^{17}O CP MAS spectra (contact time 5 ms) of isotropic ZnO NCs (Sample 1) exposed to ^{17}O water for 5 h (a), for 14 h (b) and for 33 h followed by on night of vacuum-drying (c). Inset: Evolution of residual water signals in the T_1 -filtered ^{17}O MAS spectra over time (between 20 min and 20 h) showing the shift (up to -2.6 ppm) and the appearance of a new resonance at -4.6 ppm for water signal.

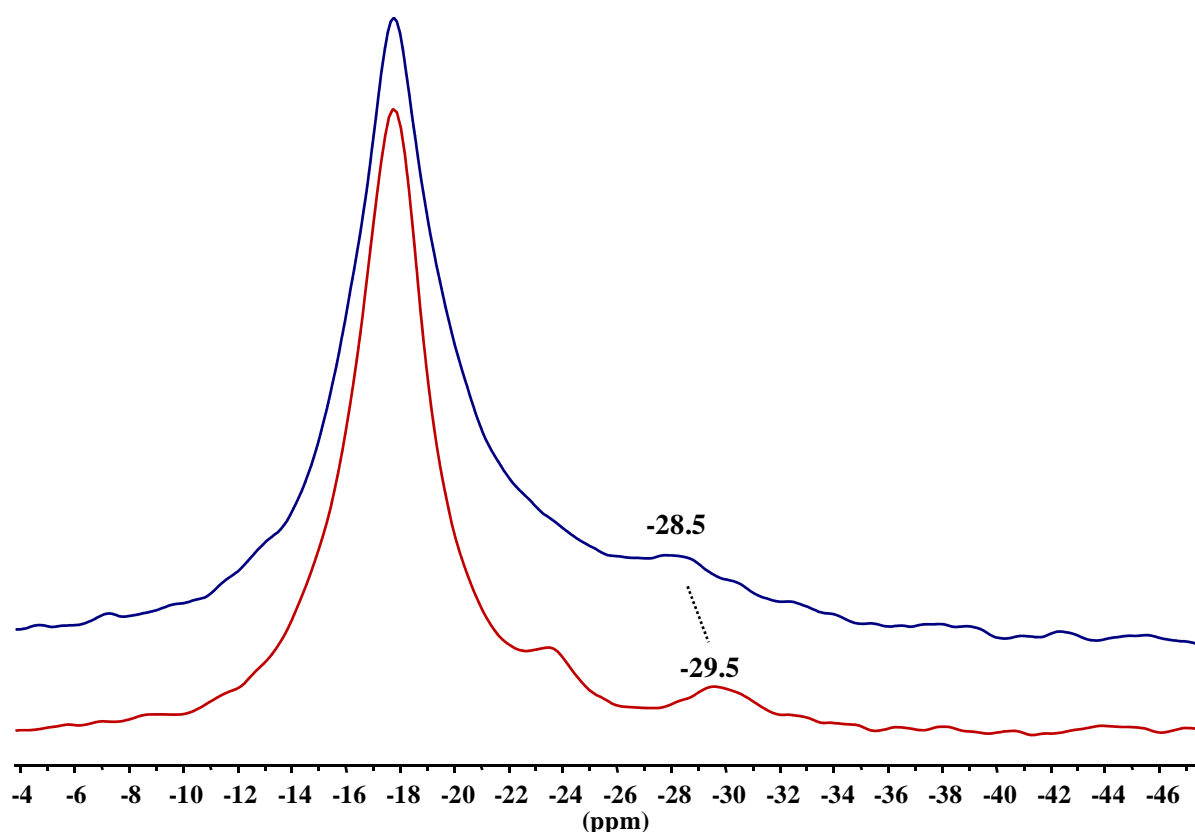


Figure S15-3: 1D T_1 -filtered ^{17}O MAS spectra (relaxation delay of 20s) in the equilibrium state of the isotope exchange experiments of isotropic ZnO NCs (Sample **1**) before (red) and after (blue) vacuum drying. A shift of the ^{17}O signal from -29.5 ppm to -28.6 ppm after the drying procedure suggests that the corresponding chemical moieties are involved in hydrogen bonds with water molecules, thus supporting the assignment of this peak area to O atoms located at the ZnO surface. Note also the shift of the medium frequency signal (at \sim -23.5 ppm) to high frequency. As it has been evidenced by XRD analysis (see below), the ZnO NCs show better crystallinity after watering/drying cycle. The removing of some of the ZnO defects and of water molecules at the ZnO surface after vacuum/drying leads to a more homogenous environment for the different ^{17}O sites. The ^{17}O sites in the first sub-layers of the NCs (medium frequency signal) show therefore chemical shifts closer to the one of the ZnO core. This results in a broadening of the ^{17}O core signal at -17.7 ppm that hinders the differentiation of the medium frequency signal from the ^{17}O core signal.

¹⁷O CP/MAS NMR of vacuum dried isotropic ¹⁷O-synthesized ZnO NCs (Sample 1') before and after exposition to unenriched water.

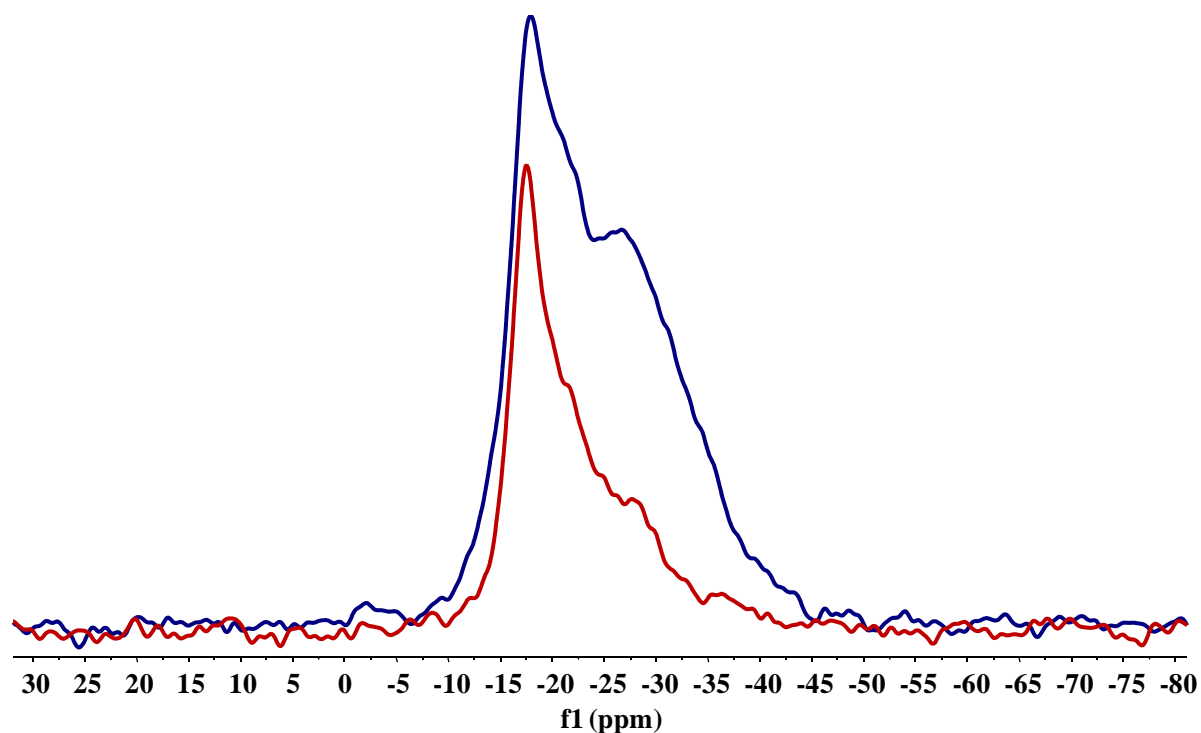


Figure S16: ¹⁷O CP/MAS spectra (contact time 5 ms) of vacuum-dried ¹⁷O-synthesized isotropic NCs (sample 1') before (blue) and after 4 days exposition to unenriched water (red).

1D T_1 -filtered ^{17}O MAS NMR spectra of isotropic (Sample 1) in the equilibrium state (step 1) and after a long unenriched water exposition-vacuum drying protocol (step 2).

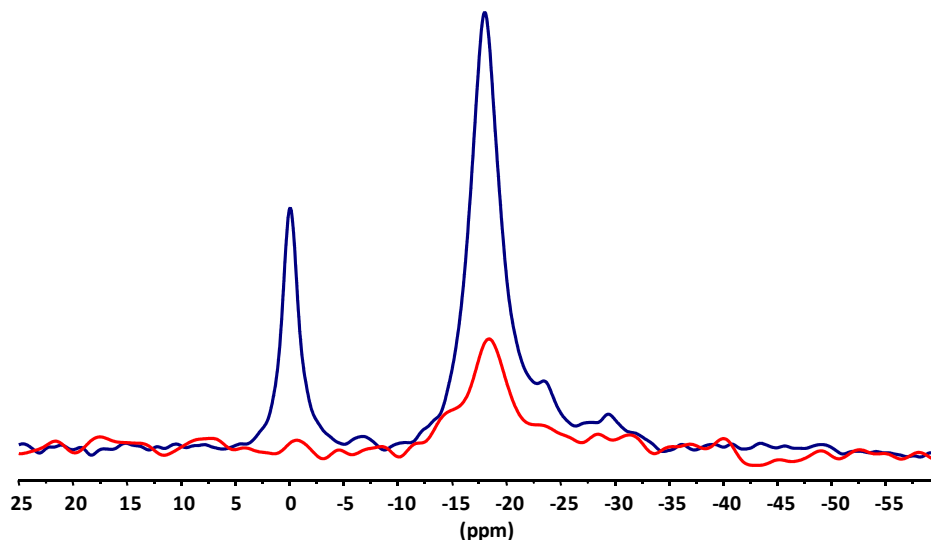


Figure S17: 1D T_1 -filtered ^{17}O MAS spectra of ^{17}O -exchanged isotropic ZnO NCs (Sample 1) in the equilibrium state of the isotope exchange experiments (step 1, blue) and after a long unenriched water exposition followed by vacuum drying protocol (step 2, red).

1D T_1 -filtered ^{17}O MAS NMR spectra of isotropic ZnO NCs submitted to 2 (Sample 3) and 6 (Sample 4) cycles of long water exposition and vacuum drying in the presence of ^{17}O -enriched water over time.

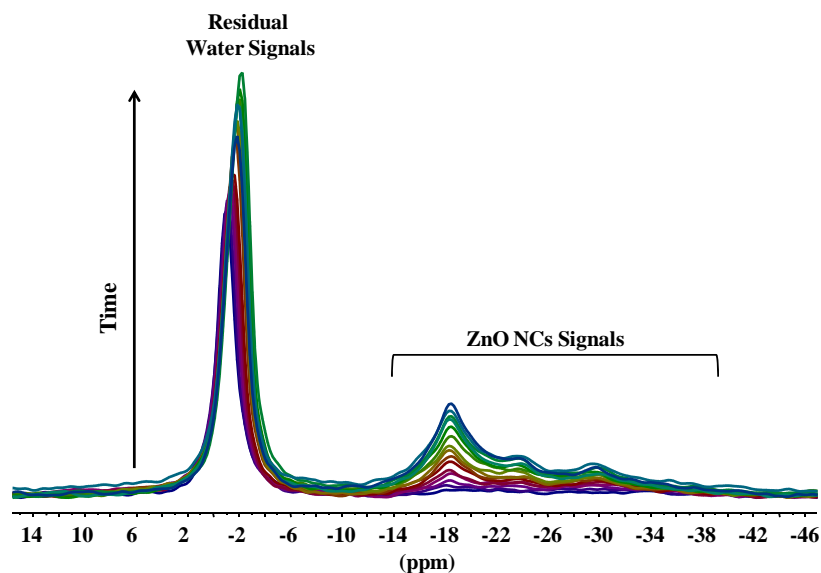


Figure S18-1: 1D T_1 -filtered ^{17}O MAS spectra of isotropic ZnO NCs submitted to 2 cycles of long water exposition and vacuum drying (Sample 3) exposed to ^{17}O -enriched water between 30 min and 47 h.

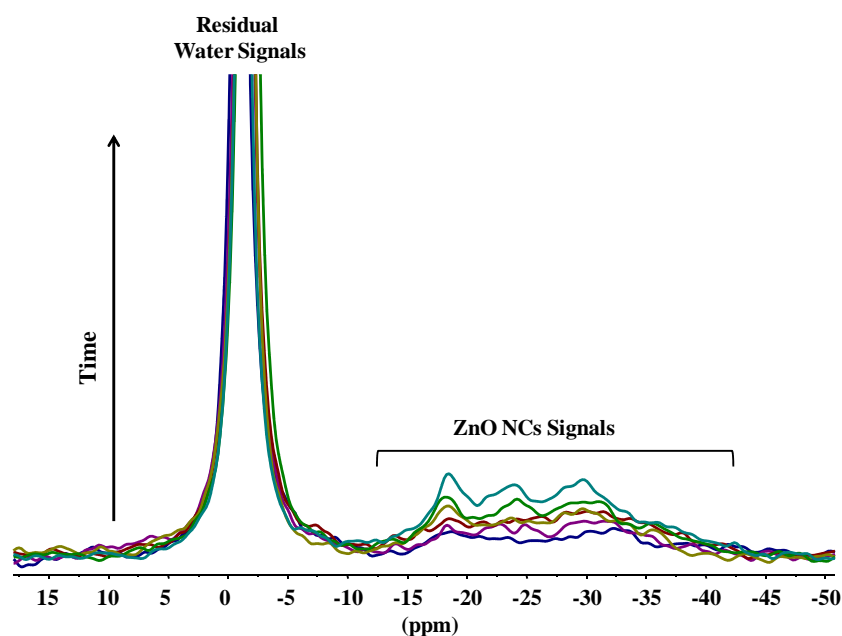


Figure S18-2: 1D T_1 -filtered ^{17}O MAS spectra of isotropic ZnO NCs submitted to 6 cycles of long water exposition and vacuum drying (Sample 4) exposed to ^{17}O -enriched water between 2.5 h and 96 h.

Superposition of 1D T_1 -filtered ^{17}O MAS spectra of ZnO NCs in the equilibrium state of the isotope exchange experiments: isotropic (Sample 1), isotropic submitted to 2 (Sample 3) and 6 (Sample 4) cycles of long water exposition and vacuum drying.

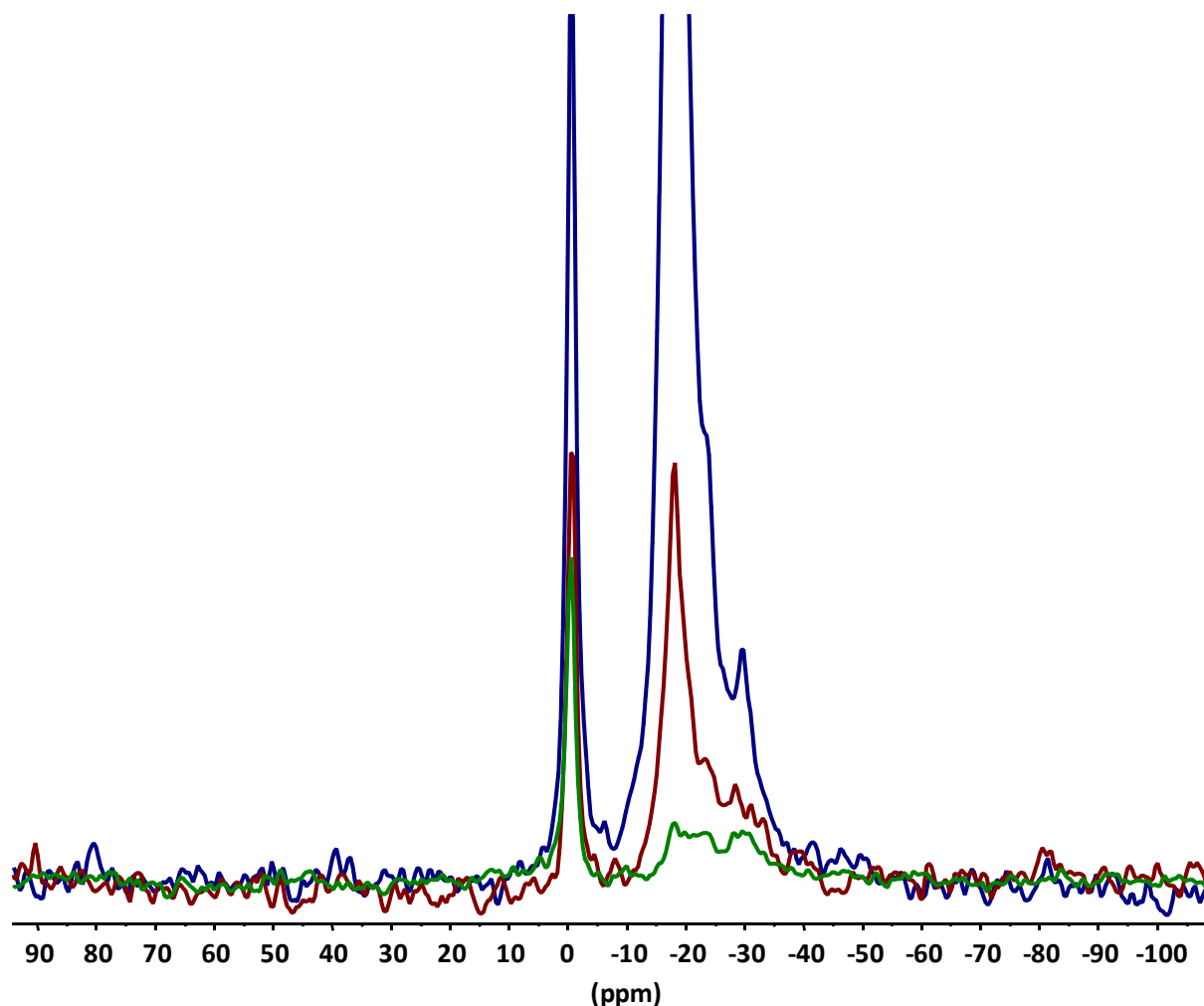


Figure S19: Superposition of 1D T_1 -filtered ^{17}O MAS spectra (relaxation delay of 20 s) of ZnO NCs in the equilibrium state of the isotope exchange experiments: isotropic (Sample 1, blue), isotropic submitted to 2 (Sample 3, red) and 6 (Sample 4, green) cycles of long water exposition and vacuum drying. Sample 1, 3 and 4 of isotropic ZnO NCs originate from the same synthesis batch.

Comparison of the global ^{17}O signal intensities (S20-1) and of the peak integrals of the -17.7 (high), -23.5 (medium) and -29.4 (low) (S20-2) of Sample 1, Sample 3 and Sample 4 in function of exposition time to H_2O -enriched in ^{17}O . The fitting curves are represented by the dashed lines (---) using the equation $I(t)=I(\infty)[1 - \exp\{-k.t\}]$.

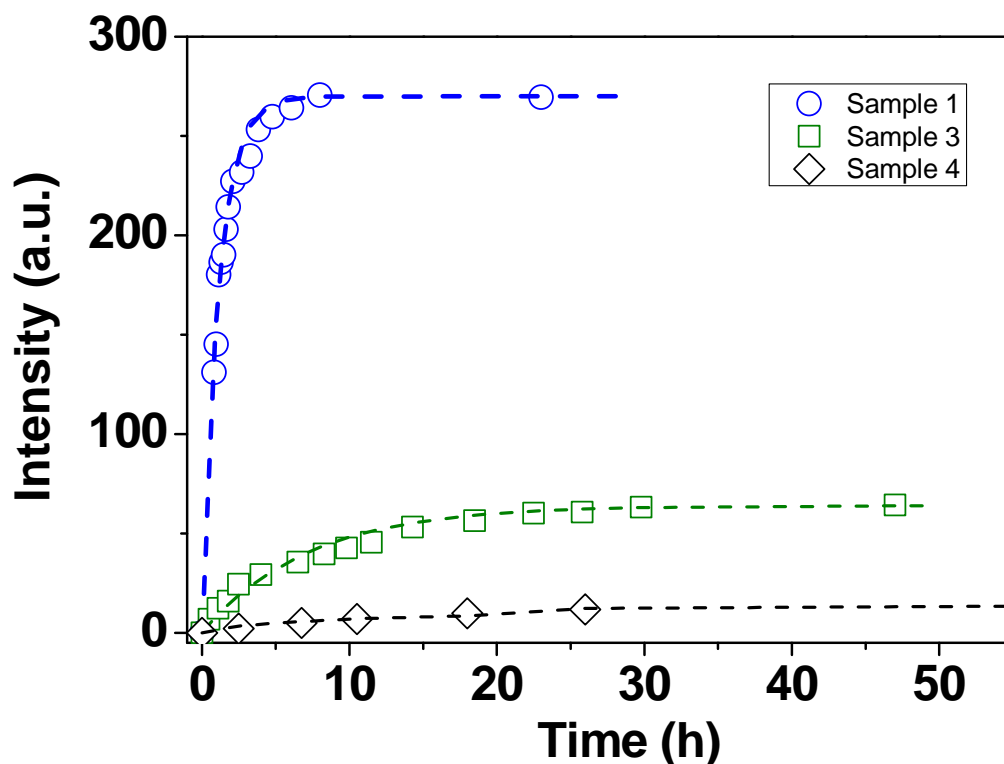


Figure S20-1: Global ^{17}O signal intensities of Sample 1 (\circ), Sample 3 (\square) and Sample 4 (\diamond) in function of exposition time to H_2O -enriched in ^{17}O . The fitting curves are represented by the dashed lines (---) using the equation $I(t)=I(\infty)[1 - \exp\{-k.t\}]$.

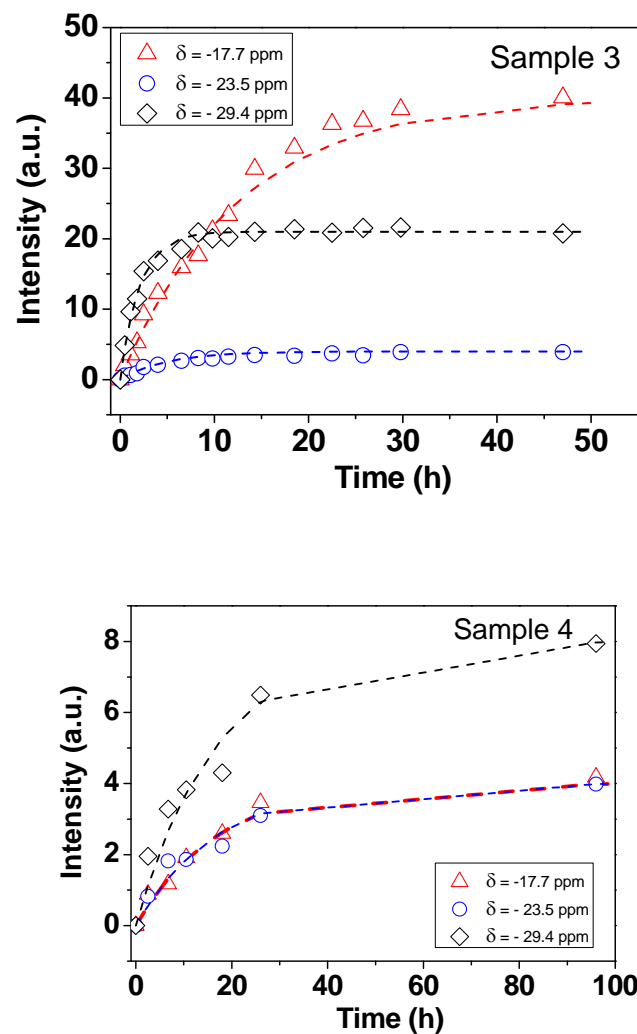


Figure S20-2: Areas $\delta = -17.7(\pm 0.1)$ ppm (high, Δ), $\delta = -23.5(\pm 0.2)$ ppm (medium, \square), $\delta = -29.4(\pm 0.2)$ ppm (low, \diamond) of Sample 3 and Sample 4 in function of exposition time to H_2O -enriched in ^{17}O . The fitting curves are represented by the dashed lines (---) using the equation $I(t) = I(\infty)[1 - \exp\{-k \cdot t\}]$. See figure S9 for sample 1.

X ray powder diffraction patterns of isotropic ZnO NCs: S21-1) just after synthesis; S21-2) after 2 watering/drying cycles; S21-3) after 6 watering/drying cycles; S21-4) full width at half maximum (FWHM) of the peaks and the corresponding coherence length of the tree patterns. TEM images of the sample just after synthesis and after 6 watering/drying cycles S21-5).

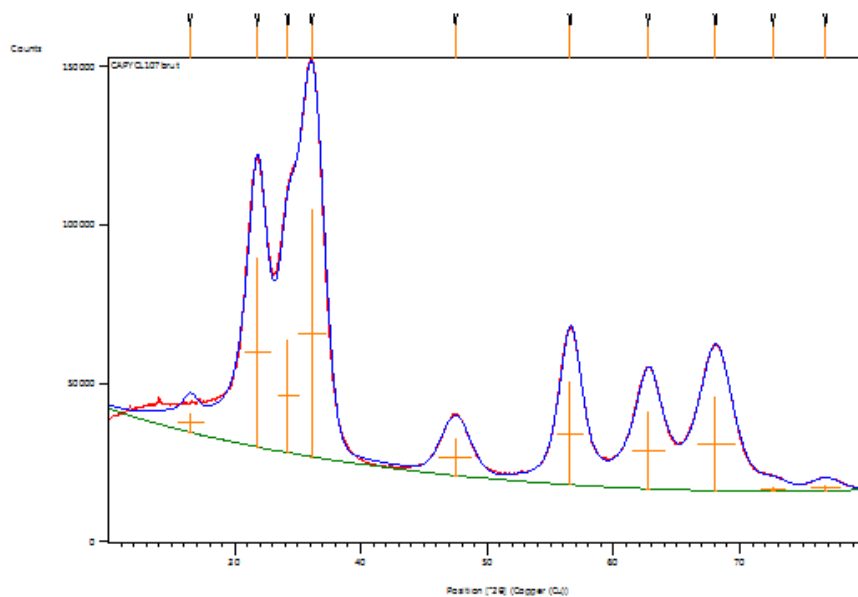


Figure S21-1: X ray powder diffraction pattern of isotropic ZnO NCs just after synthesis.

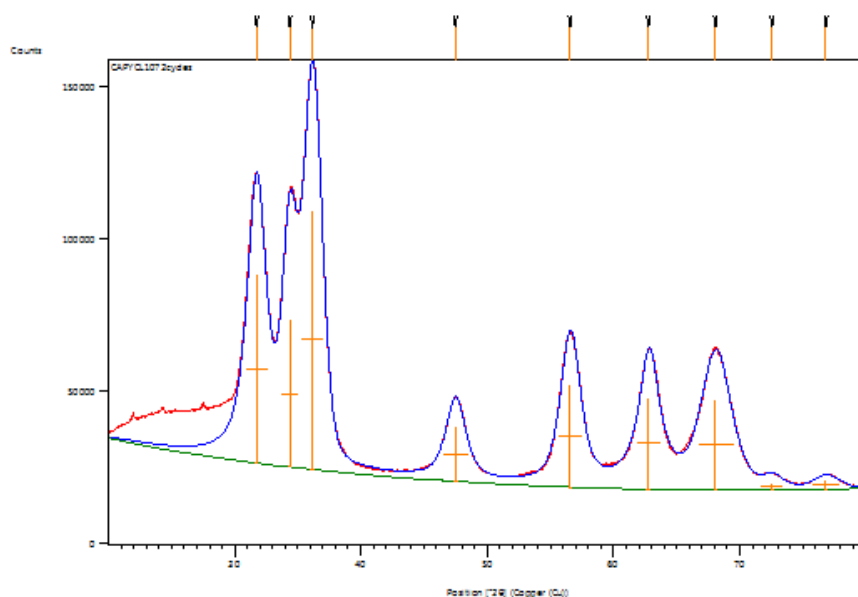


Figure S21-2: X ray powder diffraction pattern of isotropic ZnO NCs after 2 watering/drying cycles.

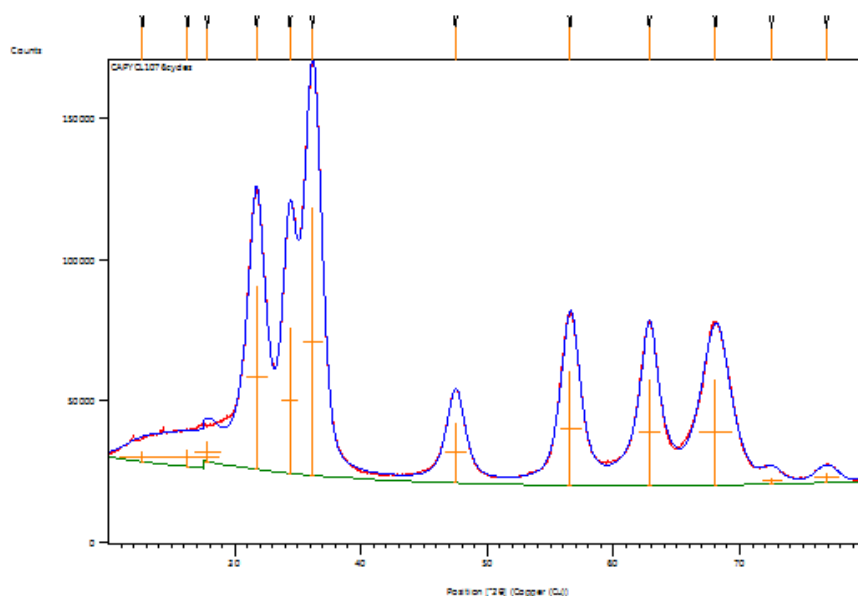


Figure S21-3: X ray powder diffraction pattern of isotropic ZnO NCs after 6 watering/drying cycles.

(hkl)	ZnO NCs	just after synthesis	after watering/drying cycles 2	after watering/drying cycles 6
(100)	FWHM (2 Θ)	2.040	1.780	1.637
	Coherence length (Å)	40	46	50
(002)	FWHM (2 Θ)	1.599	1.333	1.235
	Coherence length (Å)	52	62	67
(101)	FWHM (2 Θ)	2.144	1.692	1.577
	Coherence length (Å)	39	49	53
(102)	FWHM (2 Θ)	2.590	1.793	1.649
	Coherence length (Å)	34	48	53
(110)	FWHM (2 Θ)	2.057	1.810	1.693
	Coherence length (Å)	44	50	53
(103)	FWHM (2 Θ)	2.581	1.855	1.685
	Coherence length (Å)	36	50	55
(112)	FWHM (2 Θ)	2.972	2.705	2.590
	Coherence length (Å)	32	35	37

Figure S21-4: full width at half maximum (FWHM) of the peaks and the corresponding coherence length of the tree patterns.

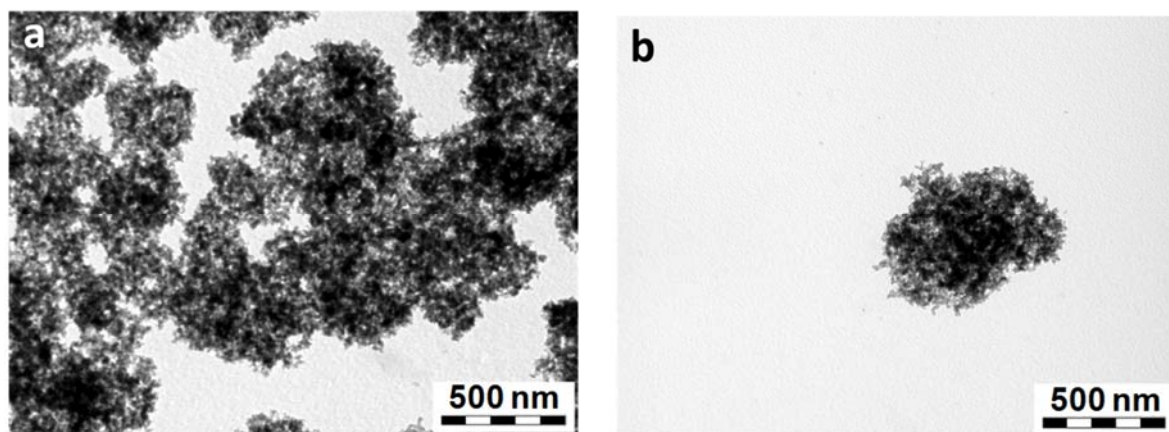


Figure S21-5: TEM images of the sample a) just after synthesis and b) after 6 watering/drying cycles. Note that the washing procedure leads to aggregation of the pristine NCs but that the watering/drying cycles do not affect the size and shape of the NCs.

- (1) Turner, G. L.; Chung, S. E.; Oldfield, E. J. *Magn. Reson.*, 1985, 64, 316
- (2) d'Espinose de Lacaillerie, J. B.; Fretigny, C.; Massiot, D. *J. Magn. Reson.* **2008**, 192, 244
- (3) Meyer, B.; Rabaa, H.; Marx, D. *Phys. Chem. Chem. Phys.* **2006**, 8, 1513.
- (4) Wang, M.; Wu, X.-P.; Zheng, S.; Zhao, J.; Li, L.; Shen, L.; Gao, Y.; Xue, N.; Guo, X.; Huang, W.; Gan, Z.; Blanc, F.; Yu, Z.; Ke, X.; Ding, W.; Gong, X.-Q.; Grey, C.P.; Peng, L. *Sci. Adv.* **2015**, 1:e1400133
- (5) Cho, G.; Wu, Y.; Ackerman, J. L. *science* **2003**, 300, 1123–1127.
- (6) Kafalak, A.; Kolodziejshi, W. *Magn. Res. Chem.*, **2008**, 46, 335-341.